Dist: A

AD-A284 213

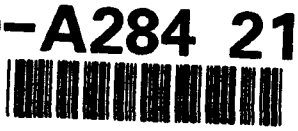

DOCUMENTATION PAGE

2. REPORT DATE	3. REPORT TYPE AND DATES COVERED
	FINAL 15 Oct 92 To 14 Feb 94

4. TITLE AND SUBTITLE

NCL(B) BASED SHORT WAVELENGTH CHEMICAL LASER

5. FUNDING NUMBERS

F49620-93-C-0003
63218C
1601/08

6. AUTHOR(S)

Dr T. T. Yang

7. PERFORMING ORGANIZATION NAME(S) AND ADDRESS(ES)

Rocketdyne Division
Rockwell International
Canoga Park, CA 91304

8. PERFORMING ORGANIZATION REPORT NUMBER

9. SPONSORING/MONITORING AGENCY NAME(S) AND ADDRESS(ES)

AFOSR/NL
110 Duncan Ave Suite B115
Bolling AFB DC 20332-0001

Dr Michael Berman

10. SPONSORING/MONITORING AGENCY REPORT NUMBER

AFOSR-TR 94 0475

11. SUPPLEMENTARY NOTES

12a. DISTRIBUTION/AVAILABILITY STATEMENT

Approved for public release;
distribution unlimited.

12b. DISTRIBUTION CODE

A

13. ABSTRACT (Maximum 200 words)

Based on the results of this work, the prospects of development of a visible chemical laser based on NCl(b) are promising. NCl, in the electronically excited b-state emits to the ground state at 665 nm. The NCl b-state is generated by energy-pooling of NCl(a) and excited iodine atoms, I*. All of these species can be generated from chemical reactions solely. This work has shown that: 1. In the generation of NCl, the branching ratio for NCl(a) is high. 65% of the HN3 ends up in the NCl(a) state. 2. The rate constant for the energy-pooling reaction NCl(a) + I*] NCl(b) is quite favorably large, approximately 10-11 cm3/sec. 3. A gain on the order of 1x10-4cm-1 was obtained. 4. Variations of the cavity ring-down experiment showed t. at virtualy no NCl(x) is formed via raction (2.6).

14. SUBJECT TERMS	15. NUMBER OF PAGES
	16. PRICE CODE

17. SECURITY CLASSIFICATION OF REPORT	18. SECURITY CLASSIFICATION OF THIS PAGE	19. SECURITY CLASSIFICATION OF ABSTRACT	20. LIMITATION OF ABSTRACT
(U)	(U)	(U)	(U)

GENERAL INSTRUCTIONS FOR COMPLETING SF 298

The Report Documentation Page (RDP) is used in announcing and cataloging reports. It is important that this information be consistent with the rest of the report, particularly the cover and title page. Instructions for filling in each block of the form follow. It is important to **stay within the lines to meet optical scanning requirements.**

Block 1. Agency Use Only (Leave Blank)

Block 2. Report Date. Full publication date including day, month, and year, if available (e.g. 1 Jan 88). Must cite at least the year.

Block 3. Type of Report and Dates Covered. State whether report is interim, final, etc. If applicable, enter inclusive report dates (e.g. 10 Jun 87 - 30 Jun 88).

Block 4. Title and Subtitle. A title is taken from the part of the report that provides the most meaningful and complete information. When a report is prepared in more than one volume, repeat the primary title, add volume number, and include subtitle for the specific volume. On classified documents enter the title classification in parentheses.

Block 5. Funding Numbers. To include contract and grant numbers; may include program element number(s), project number(s), task number(s), and work unit number(s). Use the following labels:

C - Contract	**PR** - Project
G - Grant	**TA** - Task
PE - Program Element	**WU** - Work Unit Accession No.

Block 6. Author(s). Name(s) of person(s) responsible for writing the report, performing the research, or credited with the content of the report. If editor or compiler, this should follow the name(s).

Block 7. Performing Organization Name(s) and Address(es). Self-explanatory.

Block 8. Performing Organization Report Number. Enter the unique alphanumeric report number(s) assigned by the organization performing the report.

Block 9. Sponsoring/Monitoring Agency Names(s) and Address(es). Self-explanatory.

Block 10. Sponsoring/Monitoring Agency. Report Number. (If known)

Block 11. Supplementary Notes. Enter information not included elsewhere such as: Prepared in cooperation with...; Trans. of ..., To be published in .... When a report is revised, include a statement whether the new report supersedes or supplements the older report.

Block 12a. Distribution/Availablity Statement. Denote public availability or limitation. Cite any availability to the public. Enter additional limitations or special markings in all capitals (e.g. NOFORN, REL, ITAR)

DOD - See DoDD 5230.24, "Distribution Statements on Technical Documents."
DOE - See authorities
NASA - See Handbook NHB 2200.2.
NTIS - Leave blank.

Block 12b. Distribution Code.

DOD - DOD - Leave blank
DOE - DOE - Enter DOE distribution categories from the Standard Distribution for Unclassified Scientific and Technical Reports
NASA - NASA - Leave blank
NTIS - NTIS - Leave blank.

Block 13. Abstract. Include a brief (Maximum 200 words) factual summary of the most significant information contained in the report.

Block 14. Subject Terms. Keywords or phrases identifying major subjects in the report.

Block 15. Number of Pages. Enter the total number of pages.

Block 16. Price Code. Enter appropriate price code (NTIS only).

Blocks 17. - 19. Security Classifications. Self-explanatory. Enter U.S. Security Classification in accordance with U.S. Security Regulations (i.e., UNCLASSIFIED). If form contains classified information, stamp classification on the top and bottom of the page.

Block 20. Limitation of Abstract. This block must be completed to assign a limitation to the abstract. Enter either UL (unlimited) or SAR (same as report). An entry in this block is necessary if the abstract is to be limited. If blank, the abstract is assumed to be unlimited.

NCl(b) BASED SHORT WAVELENGTH CHEMICAL LASER

FINAL REPORT

15 OCTOBER 1992 through 14 MAY 1994

Date: 14 MAY 1994
Contract : F49620-93-C-0003

Prepared for

AIR FORCE OFFICE OF SCIENTIFIC RESEARCH

by

V. T. Gylys, T. T. Yang and R. N. Hindy

Rocketdyne Division/Rockwell International
6633 Canoga Avenue
Canoga Park, California 91309-7922

NOTICE

This report was prepared as an account of work sponsored by an agency of the United States Government. Neither the United States nor any agency thereof, nor any of their employees, makes any legal warranty, expressed or implied, or assumes any liability or responsibility for any third party's use of the results or such use of any information, apparatus, product, or process disclosed in this report, or represents that its use by such third party would not infringe privately owned rights.

This report has been reproduced directly from the best available copy. All the analytical and experimental work reported here was completed by May 14, 1994.

Available from the National Technical Information Service, U. S. Department of Commerce, Springfield, Virginia 22161

TABLE OF CONTENTS

1.0 TECHNICAL REPORT SUMMARY

1.1 Project Objectives

The objective of the research described in this report is to determine the feasibility of developing a laser operating at a wavelength of 665 nm based on a chemically derived system of $NCl(b^1\Sigma)$ molecules. The lasing species $NCl(b^1\Sigma)$ is generated by energy transfer (pooling) between $NCl(a^1\Delta)$ and $I^*(^2P_{1/2})$, the latter excited by energy transfer from $NCl(a^1\Delta)$, and the former generated by the reaction of $Cl + N_3$.

1.2 Concept Description

An experimental and theoretical study of a new chemical laser operating in the visible at 665 nm has been conducted. The upper level of the lasing species is the electronically excited $b^1\Sigma$ state of the NCl molecule. $NCl(b^1\Sigma)$ is generated by energy transfer (pooling) between $NCl(a^1\Delta)$ and I^*. This system is analogous to the $NF(b^1\Sigma)$ system investigated by J. Herblin[1]. However, since the radiative lifetime for $NF(b^1\Sigma)$ is 20ms which is considerably longer than the 630 μs for $NCl(b^1\Sigma)$. and the value of the cross-section for stimulated emission is $3 \times 10^{-18} cm^3 s^{-1}$ for $NCl(b^1\Sigma)$ whereas it is on the order of $10^{-19} cm^3 s^{-1}$ for $NF(b^1\Sigma)$, this system is expected to be superior.

1.3 Accomplishments

A pyrex cylindrical fast flow reactor (CFFR) and associated hardware were assembled. Two spectrometers were mounted on a single cart which could be easily moved along the (CFFR). Each spectrometer was interfaced to an optical multichannel analyzer (OMA). Each spectrometer/OMA pair was calibrated in order to measure absolute $NCl(b^1\Sigma)$ and $NCl(a^1\Delta)$ photon yields simultaneously.

In the first phase of this work, the $NCl(b^1\Sigma)$ and $NCl(a^1\Delta)$ photon yields were measured. These measurements indicated that at least 65 percent of the NCl molecules resulting from the reaction of Cl with N_3 result in the $NCl(a^1\Delta)$ electronic state. The yield of $NCl(b^1\Sigma)$ was shown to be less than .01 percent. The high yield of $NCl(a^1\Delta)$ molecules is encouraging, not only for using this molecule to produce $NCl(b^1\Sigma)$ but also, because of its near resonance with I^*, as an energy storage source for an I^* laser.

In the second phase, experiments were carried out to measure the pooling rate coefficient of $I^*(^2P_{1/2})$ and $NCl(a^1\Delta)$ to $NCl(b^1\Sigma)$. The pooling rate was deduced by

monitoring the absolute emission intensity of NCl(b→X), NCl(a→X) and I($^2P_{1/2} \rightarrow {}^2P_{3/2}$) as a function of distance (time) down the length of the CFFR. This measurement was made with and without ICl present. The enhancement in the NCl(b→X) emission at 665 nm, when iodine atoms were present, was clearly evident. This rate was estimated to be $1 \times 10^{-11} cm^3 s^{-1}$. An alternate experiment was setup to confirm this rate. In this experiment photolysis by 248 nm photons of CF_3I and ClN_3 produced an instantaneous source of I* and NCl(a). By knowing and varying the concentrations of these two species and monitoring their time dependence as a function of number density, it was hoped that the pooling rate could be confirmed. However, the I_2(b-X) emission obscured the results and only qualitative information was obtained.

In the final phase of this contract, the CFFR was modified to accept a 1/2 meter transverse optical cavity. A cavity ring-down technique was used to make small signal gain measurements under optimized NCl(b) population conditions. A small signal gain of $1 \times 10^{-4} cm^{-1}$ was recorded. The cavity ring-down experiments also showed that virtualy no NCl(X) is produced.

1.4 Future NCl Based Laser Research

Based on the results of this research contract the prospects of development of a visible chemical laser based on NCl(b) are encouraging. The branching ratio for production of NCl(a) was found to be high (65%). Results indicate that NCl($b^1\Sigma$) can be produced from pooling of I*($^2P_{1/2}$) and NCl($a^1\Delta$) at a rate of $1 \times 10^{-11} cm^3 s^{-1}$. It is desirable to confirm this rate measurement using an alternate methology. Although the emphasis of this program has been to investigate the feasibility of producing an NCl($b^1\Sigma$) based chemical laser, the results of this research contract also indicate that NCl($a^1\Delta$) is an ideal candidate for pumping an I* laser. In the work reported here the production of NCl(a) from the reaction of N_3 and Cl was found to approach unity Furthermore, the rate constant for the reaction

$$I + NCl(a) \rightarrow I^* + NCl(X) \qquad (1.1)$$

has been recently measured to be approximately 1×10^{-10} cm^3 s^{-1}. These findings make NCl($a^1\Delta$) an attractive energy storage source for an iodine laser. Apart from the obvious advantages of a nonaqueous gas phase system, the use of isoelectronic NCl($a^1\Delta$) instead of $O_2(a^1\Delta)$ as the energy source for an iodine laser may also lead to less stringent inversion requirements. The near-resonant production of I*($^2P_{1/2}$) by reaction (1.1) results in the formation of vibrationally excited NCl($X^3\Sigma$), which is readily collisionally deactivated.

2. INTRODUCTION

The principle of a short-wavelength chemical laser is to generate, by chemical reactions, electronically-excited product molecules capable of sustaining laser action. In practice, most chemical reactions give ground electronic state products. Those that do not generally give products in their lowest lying metastable states. These states typically have small stimulated emission cross sections, and are quite low in energy (~1eV, 23Kcal/mole), making them unsuitable for visible lasing.

One way to generate higher lying electronic states is to pool the energy of two less-excited species. This has been shown in the upconversion of $NF(a^1\Delta)$ to $NF(b^1\Sigma)$ by $I^*(^2P_{1/2})$ [1]

$$NF(a^1\Delta) + I^*(^2P_{1/2}) \rightarrow NF(b^1\Sigma) + I(^2P_{3/2}) \qquad (2.1)$$

This reaction has been shown to be very efficient[1,2]. Although frequency upconversion by means of an iodine laser could be used to produce green lasing of $NF(b^1\Sigma)$, the unfavorably long radiative lifetime (t = 23 ms) [3,4] and resulting low stimulated emission cross section make the concept unattractive.[12,13] It has been suggested that the energy of $NF(b^1\Sigma)$ be collisionally transferred to a lasing molecule, such as IF.[5,6]

$$NF(b^1\Sigma) + IF(X) \rightarrow NF(X^3\Sigma) + IF(b) \qquad (2.2)$$

Unfortunately, this energy transfer is very slow while associated deactivation reactions between $NF(b^1\Sigma)$ and $IF(X^3\Sigma)$ are very fast.[7]

An attractive alternative, the $NCl(b^1\Sigma)$ molecule, is isoelectronic with $NF(b^1\Sigma)$ and has a much shorter radiative lifetime. As shown in Table 2.1 The radiative lifetimes for $NCl(b^1\Sigma)$ and $NF(b^1\Sigma)$ are 630 μs and 23 ms, respectively.[3,8,10] The estimated gain cross-section for $NCl(b^1\Sigma)$ is 3×10^{-18} cm^2. This value is comparable to 7.4×10^{-18} cm^2 for $I^*(^2P_{1/2})$.[11]

In order to better understand several possible laser systems based on energy storage in $NF(a^1\Delta)$ many studies have been made concerning the production of as well as the rates and mechanisms of energy transfer processes involving the excited $a^1\Delta$ and $b^1\Sigma^+$ states of the NF radical.[1-5,12] However, relatively little is known about these states for the analogous NCl molecule, although it too can be produced efficiently from reactions of azides.

Interest in mechanisms for the production of as well as the reaction kinetics of the $a^1\Delta$ and $b^1\Sigma^+$ states of NCl has recently resurfaced with the results of Bower and Yang[14,15] suggesting the possibility of using $NCl(a^1\Delta)$ to pump an I^* laser and the suggestion of Yang and Gylys[16] of using an energy pooling reaction of $NCl(a^1\Delta)$ with I^* to pump an NCl(b) laser (665nm). Yang and Bower described the large valve (1×10^{-10} cm^3s^{-1}) for the rate constant of the NCl(a) + I energy transfer to be associated with the operation of a near resonant energy-transfer process

$$NCl(a,v=0) + I(^2P_{3/2}) \rightarrow NCl(X,v=2) + I^*(^2P_{1/2}) + 50\ cm^{-1}. \qquad (2.3)$$

Ray and Coombe[20], using photolysis at 193nm to produce iodine atoms and NCl($a^1\Delta$) respectively have determine the NCl(a) - I energy transfer rate to be somewhat slower (1.8 x $10^{-11}cm^3s^{-1}$). Although there is some disagreement between the two reported rate measurements, the potential of an NCl(a) pumped I* laser is very promising. A source of electronically excited nitrene (NX) molecules has been shown to be the reaction

$$X + N_3 = NX(a,B) + N_2 \qquad (2.4)$$

Where X is a halogen atom. The determination of this branching ratio was one of the objectives of this research contract. However, based on the analogous NF system it was believed that the major excited species excited is the lower lying NCl($a^1\Delta$) state. This lead to our proposal to investigate a new visible chemical laser based on excited NCl($b^1\Sigma$) molecules. The proposed chemical reaction sequences for NCl($b^1\Sigma$) formation are as follows:

$$Cl + HN_3 \rightarrow HCl + N_3 \qquad (2.5)$$
$$Cl + N_3 \rightarrow NCl\ (a^1\Delta, b^1\Sigma, X^3\Sigma) + N_2 \qquad (2.6)$$
$$NCl(a^1\Delta) + I(^2P_{3/2}) \rightarrow NCl(X^3\Sigma,\ v = 2) + I^*(^2P_{1/2}) + 50\ cm^{-1} \qquad (2.7)$$
$$NCl(a^1\Delta) + I^*(^2P_{1/2}) \rightarrow NCl(b^1\Sigma,\ v = 2) + I(^2P_{3/2}) + 10\ cm^{-1} \qquad (2.8)$$
$$NCl\ (b^1\Sigma,\ v = 2) + M \rightarrow NCl(b^1\Sigma,\ v = 0) + M \qquad (2.9)$$
$$NCl(X^3\Sigma) + NCl(X^3\Sigma) \rightarrow N_2 + 2\ Cl \qquad (2.10)$$
$$NCl(b^1\Sigma) \rightarrow NCl(X^3\Sigma) + 665\ nm \qquad (2.11)$$

The energy diagrams of NCl($a^1\Delta$), NCl($b^1\Sigma$) and $I^*(^2P_{1/2})$ are shown in Figure 2.1. As seen in this diagram, the NCl($b^1\Sigma$, v = 2) state is in near resonance with NCl($a^1\Delta$) + $I^*(^2P_{1/2})$. Determination of the transfer rate of reaction (2.8) was another goal of this contract. Based on some preliminary flow tube experiments, which showed a significant enhancement of NCl($b^1\Sigma$) emission when $I(^2P_{1/2})$ atoms were present, it was expected to be efficient. The dashed curve of Figure 2 shows the emission spectrum resulting from the reaction of Cl + HN_3. The emission is mainly due to (0,0) band of the b→X transition. The solid curve in Figure 2.2 shows the spectrum obtained with addition of ICl at a density of 1 x $10^{13}/cm^3$ to the Cl/HN_3 flow field. This resulted in approximately a 250% increase in NCl(b→X) emission. Moreover, the spectrum remained dominated by the (0,0) band transition at 665 nm.

The behavior of the NCl($b^1\Sigma \rightarrow X^3\Sigma$) emission has been studied as a function of HN_3 and ICl concentrations, to gain information about the kinetic processes involved in the underlying pumping energy transfer and pooling reactions. The dependence of the observed 665 nm emission on the HN_3 concentration is plotted in Figure 2.3 for ICl concentrations 0, 5 x $10^{12}/cm^3$ and 7 x $10^{12}/cm^3$. Note that the [NCl($b^1\Sigma$)] production without ICl injection increases almost linearly with [HN_3]. The addition of ICl causes

the $NCl(b^1\Sigma)$ emission to increase with increasing HN_3 at a much higher rate. The enhancement of $NCl(b^1\Sigma)$ production varies from 200 to 250%, depending on ICl concentration, at high $[HN_3]$. These results suggested that it may be possible to convert large concentrations of electronically excited $NCl(a^1\Delta)$ radicals into the more energetic $NCl(b^1\Sigma)$ radicals by energy transfer collisions with electronically excited iodine atoms.

Determination of the NCl(a)/NCl(b) branching ratio depicted by reaction (2.6) will be discussed in section 3. The derivation of the NCl(a) + I* pooling rate constant depicted by reaction (2.8) will be shown in section 4. Finally, results of a cavity ring-down experiment determining the gain for the NCl(b) system will be presented in section 5.

3. PHOTON YIELD MEASUREMENT

3.1 Background

A number of experiments performed in recent years[12,17,18] have demonstrated that electronically excited nitrogen halide diatomics (NX = NF, NCl, NBr) can be efficiently produced by reactions between halogen atoms and small covalently bound azides,

$$X + N_3 = NX(a,b) + N_2 \qquad (3.1)$$

where X is a halogen atom. The first such experiments were reported by Clark and Clyne,[18] who observed the generation of $NCl(b^1\Sigma^+)$ and $NBr(b^1\Sigma^+)$ in reactions of chlorine or bromine atoms with ClN_3. These excited species radiate in the visible in transitions to the ground ($^3\Sigma^-$) states. Clark and Clyne showed that the excited nitrenes are produced by reactions of Cl or Br atoms with gas phase azide N_3 radicals by directly monitoring the N_3 in the reaction medium via the well-known absorption transition near 272 nm. Coombe et al,[12] showed that the reaction (3.1) can be thought of as proceeding via a halogen azide-like intermediate.

In their investigations of the reactions of halogen atoms with gaseous HN_3 Coombe et al[12], suggested that reactions such as (3.1) are strongly constrained by conservation of spin angular momentum and therefore most likely proceed via a halogen azide-like intermediate geometry, where the only accessible potential energy surface is a singlet. This singlet intermediate configuration can correlate to NX + N_2 (both singlets) or NX + N_2 (both triplets). Coombe et al[12] postulated that since the lowest-lying triplet state of N_2 is not accessible by these reactions, the yield of excited singlet NX is probably very high, as long as nonadiabatic curve crossings in the exit channel are not efficient. In the low-density limit, the yield of $NF(a^1\Delta)$ was found by Coombe and co-workers to be near unity. The yields of the $b^1\Sigma^+$ states of NCl and NBr was estimated to have a lower limit of 10 percent. However, they were not able to determine the yield of the $NCl(a^1\Delta)$ state because at the time the spontaneous emission rate for this

transition was unknown, hence direct calculation of the peak density of excited states was not possible. Furthermore, the $a^1\Delta$ - $X^3\Sigma^-$ emission signal was much to weak at the low reagent densities to be monitored by their detection system.

3.2 Experiment

Cl-HN_3 flames were produced in a cylindrical fast flow reactor (CFFR). The reactor was 5cm in diameter and approximately 1.5 meters long. It is made of pyrex and coated with halocarbon wax in order to minimize halogen atom recombination at the surface. The CFFR was equipped with an inner slide injector of concentric design. This injector could be moved to change the position of the reagent zone with respect to the fixed Cl injector. The inner slide tube was terminated in a radial array of small holes through which the HN_3 enter the CFFR. Cl atoms were produced by passage of Cl_2 diluted in Ar through a 1000W microwave discharge, which was positioned on a sidearm of the CFFR. A schematic of the experimental setup is shown in Figure 3.1.

The HN_3 was kept in 5 liter pyrex bulbs. Its rate of flow into the CFFR was controlled and monitored with an MKS flow meter. The HN_3 was prepared several days prior to experimental tests by the reaction of NaN_3 with stearic acid, $(CH_3(CH_2)_{16}$ COOH). These reagents were mixed in a ratio of 1:20 (by atomic weight) and left in vacuo overnight. Heating of the cell to approximately 50°C for 1-2 hours and then to 110°C resulted in evolution of HN_3. The gas was collected in 5 liter storage bulbs at pressures below 100 Torr. It was immediately diluted with 1000 Torr of Argon. The HN_3 could be stored this way for several months without any noticeable decomposition. In most of these experiments the HN_3 was injected into the CFFR via the sliding injector 20 cm downstream of the Cl inlet, which corresponds to a flow time of 25ms.

The spectral emissions were monitored by means of two Optical Multichannel Analyzers (OMA), each was interfaced to an Instruments SA Inc., 1/3 meter spectrometer. Both spectrometers were mounted on a single cart which could be easily positioned at any point down the length of the CFFR. This permitted the spatial and thus temporal dependence of the emissions to be obtained. The spectrometer used to monitor the NCl(a) emission in the NIR was equipped with a 600 groove/mm grating blazed at 1.0μm. The NIR OMA had a quantum, efficiency of 60 percent at the NCl(a) emission wavelength of 1.08μm. The visible emissions were dispersed by a 1200 g/mm grating blazed at 500 nm and defected with a visible OMA which has a quantum efficiency of 16 percent at the NCl(b) wavelength of 665 nm.

The light collection efficiency of each detector, hence the calibration factors, α, were obtained prior to the branching ratio experiments. The calibration factor for the visible detection system at 665nm was obtained by using the O + NO reaction as a chemical actinometer. A known concentration of a oxygen atoms were produced by the N + NO chemiluminescent titration, the N atoms were generated by passage of N_2 through a microwave discharge. At the point at which the N_2 recombination emission disappears the oxygen atom concentration is known by reading the flow rate of NO. It can

be seen from Figure 3.2 that [O] = $1.045(10^{14})cm^{-3}$. Further addition of NO to the system beyond the end point of the titration produced the yellow-green NO_2 afterglow characteristic of the O + NO reaction. The absolute photon yield of this reaction and the spectral distribution of the NO_2 emission are well known[19], (see Table 3.1) and therefore permit determination of the parameter $\alpha(665nm)$ which when multiplied by the measured intensity (photon-count rate) gives the absolute photon emission rate per cm^3.

$\{\alpha(665nm)\}(counts/sec) = K_c[O][NO]$

were $K_c = (7.5(10)^{-17}cm^3\mu m^{-1}sec^{-1})$ (BW) see Table 3.1

$(\alpha)5.67(10^2)counts/sec=\{7.5(10)^{-17}cm^3\mu m^{-1}sec^{-1}\}(BW)[6.73(10^{13})cm^{-3}][1.3(10^{14})cm^{-3}]$

where BW is the bandwidth =.016μm

$\alpha(665nm) = 1\ count = (1.85x10^7)\ photons/cm^3$

The calibration factor, α, depends on the spectral bandwidth of the spectrometer and wavelength. The photon yield measurements were made with the slits of the spectrometer opened such that the spectral width was greater than the bandwidth of the emission feature measured.

Although the NO_2 recombination emission extends to the NIR, the emission at 1.08μm was not strong enough to calibrate the IR OMA which was used to monitor the $NCl(a^1\Delta)$ emission. The absolute calibration factor $\alpha(1.08\mu m)$ for the NIR OMA was obtained by measuring the NIR photon emission rate per cubic centimeter from a known amount of $O_2(a^1\Delta)$. In the $O_2(a^1\Delta)$ molecule, the electrons are paired so the spin is zero, but the orbital angular momentum is not. Therefore the absolute amount of $O_2(a^1\Delta)$ can be measured using electron spin resonance and compared to the emission intensity obtained with the IR OMA. Figure 3.3 shows the change in IR OMA signal counts as a function of $O_2(a^1\Delta)$ partial pressure as measured by electron spin resonance. From the slope we obtain $\alpha(1.08\mu m) = 8.29x10^8$ photons/cm^3·count. All gas flow rates were monitored by using MKS mass flow meters calibrated against known N_2 flow rates. Flow rates of the gases used in the experiments were determined from conversion factors supplied by MKS.

The flow rate of Cl atoms was determined using two different methods by titration with NOCl. In the first method a mass-spectrometer was used to monitor the production of both NO and Cl_2 as NOCl was added to the Cl atoms in the flow stream. The titration point at which the production of NO and Cl_2 stopped to increase with increasing NOCl concentration indicated the Cl atom concentration (see Figure 3.4). In the second method, the Cl atom concentration was determined by monitoring the NCl(b) emission as NOCl was added to the flow stream. The NOCl was added to the flow stream prior to the injection of the HN_3. The flow rate of NOCl at which the NCl(b) emission disappeared indicated the Cl concentration. Figure 3.5 shows that with a Cl_2 flow of 30 sccm through

the microwave discharge, $4.6x10^{13}cm^{-3}$ of Cl atoms were produced. The latter method was used more often because of its ease.

3.3 Photon Yield Measurement Results

The flame of the Cl + HN_3 reaction is dominated by intense emission from the excited $a^1\Delta$ and $b^1\Sigma^+$ electronic states of NCl. As shown in Figure 3.6a, at least 90 percent of the NCl ($b^1\Sigma^+ \rightarrow X^3\Sigma^-$) emission occurs in the $\Delta v = 0$ sequence at 665 nm, giving the flame a deep red color. Previous experiments on this system indicated the pumping reaction Cl + N_3 is sufficiently exothermic for production of $NCl(b^1\Sigma^+)$, whereas F + N_3 cannot produce $NF(b^1\Sigma^+)$. It can only be produced by pooling reactions of I* with $NF(a^1\Delta)$. Emission from $NCl(a^1\Delta)$ is also observed. As shown in Figure 3.7a, the most intense bands (the $\Delta v = 0$ sequence) occurred at 1.08μm.

The photon yield measurements for the $b \rightarrow X$ and $a \rightarrow X$ transitions were complicated by three factors. First, the flow time (distance) necessary for complete mixing of the reactants must be considered from the point of injection. Second, the time length of the flame at standard conditions 1 atm pressure, is very short. Such that calibration by comparison to the O + NO system would be difficult. Third, the radiative lifetime for the $NCl(a^1\Delta)$ state is very long (1.4 sec) compared to that for NCl(b) (630 μs). Due to its relatively long radiative lifetime $NCl(a^1\Delta)$ can under go many collisions before radiating, therefore, its effective lifetime is considerably shorter than its radiative lifetime.

Figure 3.6b shows the buildup and decay in NCl(b) fluorescence intensity at 665 nm as a function of flow time from the point of injection The open and closed circles represent data taken in separate experiments under identical conditions. Each data point represents the area integrated under the spectrum in 30 seconds. The line shows the best fit to the data of the double exponential curve fitting routine. Figure 3.6a shows a typical data point(spectrum) obtained 15 cm down stream of the HN_3 injector. Since $NCl(b^1\Sigma^+)$ has such a short radiative lifetime, collisional quenching effects were ignored. The exponential decay in fluorescence intensity corresponds to the decrease in production of $NCl(b^1\Sigma^+)$ as a function of distance from the point of injection. Careful observation of the emission in the flow field indicated that complete mixing occurred within 2 cm of the injection point. This corresponds to a flow time of 2.5 ms.

Similarly, Figure 3.7b illustrates the data obtained for the buildup and decay of NCl(a→X) emission intensity at 1.08 μm. The open and closed circles represent data taken in two separate tests under identical conditions. The data points represent the integrated counts (in 12 seconds) obtained at each location along the CFFR. Figure 3.7a shows a typical data point(spectrum) obtained down stream of the HN_3 injector. The line in Figure 3.7b indicates the best fit of the double exponential curve fitting routine to the data. The rising exponential was assumed to be influenced by collisional quenching of the $NCl(a^1\Delta)$ and the distance (time) needed for complete mixing of the injected HN_3 with

reactants in the flow stream In order to determine the collisional quenching rate for $NCl(b^1\Sigma^+)$, the 2.5 ms needed for mixing as determined from the NCl(b) data was subtracted from the time constant for the rising exponential as determined by the fitting program. As shown in Figure 3.7 the collisional quenching rate was thus determined to be 1/2.5ms. In order to minimize the effects of collisional quenching and to stretch the time length of the NCl flame down the length of the CFFR, photon yield measurements were made under very low reagent concentrations. Under these conditions the collisional quenching of the excited species is minimized and the time-integrated intensity profile will approach the photon yield which can be calculated when the radiative lifetime and the effective lifetime are considered.

Flames stretching down the length of the CFFR were obtained for halogen atom densities less than 3.0 mTorr and HN_3 densities less than 0.3 mTorr. The photon yield is given by the following expression.

$$\text{Yield } NCl(b^1\Sigma^+) = \alpha(665nm) \int I(t)\, dt \bullet (1/K_r)/[HN_3] \qquad (3.2)$$

where $\alpha(665nm)$ is the detector calibration factor at the NCl(b-X) transition and I(t) is the distance (time) dependent $NCl(b \rightarrow X)$ intensity. A small component of the buildup in intensity of the $b \rightarrow X$ emission shown in Figure 3.6 is due to the mixing rate because the radiative lifetime is relatively short (630μs).

Due to its relatively long radiative lifetime (1.4 sec), NCl(a) can under go many collisions before radiating and therefore collisional quenching must be accounted for. The time decay profile of NCl(a) emission intensity can be used to deduce a total pseudo-first-order decay rate $K_d = K_r + \Sigma k_Q$ is the total quenching rate. Where K_r is the radiative loss rate and K_Q is the rate due to collisional quenching. The corrected $NCl(a \rightarrow X)$ yield is then obtained by multiplying the measured photon yield by a factor of K_d/K_r. The NCl(a) photon yield is then given by

$$\text{Yield } NCl(a^1\Delta) = \alpha(1.08\mu m) \int I(t)\, dt \bullet (K_d/K_r)/[HN_3] \qquad (3.3)$$

By knowing the flow speed (800 cm/sec) in the fast flow reactor, the buildup and decay in time of both $NCl(a^1\Delta)$ and $NCl(b^1\Sigma^+)$ were determined. By integrating under the curve shown in Figure 3.6b, using the value for $\alpha(665nm)$ derived in section 3.2 and applying equation (3.2) the $NCl(b^1\Sigma^+)$ photon yield was determined to be

$$\text{Yield } NCl(b^1\Sigma^+) = 6320x(1.85x10^7)/(4.8x10^{12})(1/1587) = .0014\%$$

Similiarly, by integrating under the curve shown in Figure 3.7b, using the value for $\alpha(1.08\mu m)$ derived in in section 3.2 and applying equation (3.3) the $NCl(a^1\Delta)$ photon yield was determined to be

$$\text{Yield } NCl(a^1\Delta) = 27x(8.29x10^8)/(4.8x10^{12})(1.4/0.010) = 65\%$$

These results indicate that at least 65% of the HN_3 molecules entering the flow stream end up in the $NCl(a^1\Delta)$ state. The fraction ending up in the b electronic state was found to be extremely small (~ .001%). These results show that large amounts of $NCl(a^1\Delta)$ can be produced via reaction (2.6).

4. DERIVATION OF THE ENERGY-POOLING RATE CONSTANT

The feasibility of developing a short wavelength chemical laser based on emission from the $NCl(b^1\Sigma^+)$ state depends upon the two critical reactions (2.7) and (2.8). For convenience these are written below:

$$NCl(a) + I \rightarrow NCl(x) + I^* \qquad (2.7)$$

$$NCl(a) + I^* \rightarrow NCl(b) + I \qquad (2.8)$$

Reaction (2.7) which has recently been studied by Yang and Bower[14,15], is analogous to the well-known pumping[11] of I* by $O_2(a^1\Delta)$ while reaction (2.8) is similar to the well known $NF(a^1\Delta)$ and I* pooling reaction system investigated by Herbelin[1,2]. Under suitable conditions it is hoped that these energy transfer processes may lead to lasing on the $NCl(b\rightarrow X)$ transition at 665nm. Since the $NCl(b\rightarrow X)$ transition is optically forbidden it may also become inverted at reduced metastable concentrations that do not lead to self-annihilation. The reverse process for reaction (2.7) was not considered because, like NF(X), the triplet ground state NCl(X) molecules are believed to be highly reactive and therefore chemically self-annihilate at a near gas kinetic rate.[1,2] Thus the NCl(X) concentration (and the rate of back reaction with I*) is reduced to insignificant values.

The experimental setup used to measure the pooling rate of reaction (2.8) was similiar to that used in determining the photon yield (described in section 3.2) except with the addition of an ICl inlet. The pooling rate, $K_{(2.8)}$, was measured by monitoring the absolute emission intensity of $NCl(b\rightarrow X)$, $NCl(a\rightarrow X)$ and $I(^2P_{1/2} \rightarrow {}^2P_{3/2})$ as a function of distance (time) down the length of the CFFR. This measurement was made with and without ICl present in order to derive the pooling rate. As shown in Figure 4.1, the enhancement in the $NCl(b\rightarrow X)$ emission at 665 nm when iodine atoms were present was clearly evident. An estimate of the pooling rate constant, $K_{(2.8)}$, for reaction (2.8)

was accomplished by considering the rate equations for the production and loss mechanism of NCl(b), and assuming a steady-state approximation:

$$\frac{d[NCl(b)]}{dt} = K_{(2.8)}\,[I^*]\,[NCl(a)] \qquad \text{PRODUCTION}$$

$$\frac{d[NCl(b)]}{dt} = K_{Rad}\,[NCl(b)] + K_{Cl2}[Cl_2]\,[NCl(b)] \qquad \text{LOSS}$$

Assuming steady-state conditions, and that quenching by molecular chlorine is the major quenching loss term, we can solve for $K_{(2.8)}$:

$$K_{(2.8)} = \frac{[NCl(b)]}{[I^*]\,[NCl(a)]}\,\{K_{Rad} + K_{Cl2}\,[Cl_2]\}$$

The values

$$[NCl(b)] = 8\times10^{8}cm^{-3}$$

$$[I^*] = 2.5\times10^{12}cm^{-3}$$

$$[NCl(a)] = 9\times10^{10}cm^{-3}$$

$$[Cl_2] = 8\times10^{13}cm^{-3}$$

were determined from the data shown in Figure 4.1.The value $K_{Rad} = 1/630\mu s = 1587\ s^{-1}$ is well known. The value for K_{Cl2} has not been measured. However, if the rate for Cl_2 quenching of NF(b) is used then $K_{Cl2} = 1.5\times10^{-11}\ cm^3s^{-1}$ and a value of

$$K_{(2.8)} \sim \frac{8\times10^{8}cm^{-3}\ \{1587\ s^{-1} + 1200s^{-1} + ..\}}{(2.5\times10^{12}cm^{-3})(9\times10^{10}cm^{-3})}$$

$$K_{(2.8)} \sim 1\times10^{-11}\ cm^3s^{-1}$$

is derived for the energy-pooling reaction. This number is comparable to that found for the corresponding reaction generating NF(b) from NF(a) and I*.

5. DERIVATION OF THE GAIN COEFFICIENT AND OBSERVATION OF GAIN

From the known value for the radiative decay, and the estimated concentration of NCl(b) in the CFFR, under a given set of operating conditions, it is possible to estimate the gain-coefficient per unit path length for the NCl(b)→NCl(X) transition at 665 nm, the [0-0] band. The gain-coefficient was determined to be

$$\alpha \sim 2 \times 10^{-4}\ cm^{-1}$$

Efforts were made to observe gain in this system employing the Cavity Ring-Down technique[21]. The essential features of this method are illustrated in Figure 5.1. As shown, a high-finesse 0.5m Fabry-Perot etalon is inserted into the flow tube by means of a vacuum-tight Pyrex glass cross. The high-reflectivity confocal etalon mirrors are mounted rigidly in a Burleigh mount with coupling to the flow-tube isolated though use of stainless-steel bellows. The high reflectivity dielectric coating of the mirrors is protected from the corrosive chemical flow by means of an argon purge. The output from an excimer-driven dye laser, tuned to the 0--0 band of the NCl(b → X) transition is directed through the confocal etalon to a filtered photomultiplier tube. The output of the PMT is observed and recorded by a fast digital storage oscilloscope. From the scope trace the decay time of the cavity is measured. Typical decay times that we have measured are in the range 3000 nanoseconds corresponding to 900 round trip passes through the optical cavity. For a gain measurement, this cavity decay time is compared, with and without the presence of NCl(b), the anticipated active laser media. If the media generates gain on the probing laser pulse, the decay time of the laser cavity will be increased, and comparison of the two traces should so indicate.

A pair of traces recorded in the absence (lower trace) and in the presence (upper trace) of NCl(b) on a logarithmic scale is shown in Figure 5.2. The small increase in decay time for NCl(b) indicates that the system may indeed have gain. The gain,α, for this system can be derived from the expression

$$ln\ (I_{on}/I_{off}) = \alpha LN \qquad (5.1)$$

were I_{on} and I_{off} are the values of the 665 nm intensity as recorded from the PMT with the HN_3 flow turned on. and off respectively, L is the length of the gain region and N is the number of passes that occured through the gain media for the cavity ring-down time at which the intensity values, I_{on} and I_{off}, are compared. Figure 5.2 shows that for a cavity ring-down time of 2.85 μs (which corresponds to 1710 passes through the gain region), I_{on} = 3.68 while I_{off} = 3.60. Substituting these values into equation (5.1) gives

$$\alpha L = (1710)^{-1} \ln(e^{3.68}/e^{3.60})$$

$$\alpha L = 4.68 \times 10^{-5}$$

If L is between .25cm and 0.5cm then

$$\alpha \sim 1.87 \times 10^{-4} cm^{-1} \text{ to } 9.35 \times 10^{-5} cm^{-1}$$

Tests were also conducted in which the HN_3 mass flow as well as reactant concentrations were varied. The value of α in these tests was always found to be positive. These experiments confirm the branching ratio results presented in section 3.3 and imply that the ammount of $NCl(X^3\Sigma)$ produced via reaction (2.6) is insignificant. These results suggest that reaction (2.6) behaves similiarly to the analogous reaction studied by Coombe et al[12] in NF and is strongly constrained by conservation of spin angular momentum and proceeds via a halogen azide-like intermediate geometry, where the only accessible potential energy surface is a singlet. These results also imply that the nonadiabatic curve crossings in the exit channel are not efficient.

6. CONCLUSIONS

Based on the results of this work, the prospects of development of a visible chemical laser based on NCl(b) are promising. NCl, in the electronically excited b-state emits to the ground state at 665 nm. The NCl b-state is generated by energy-pooling of NCl(a) and excited iodine atoms, I*. All of these species can be generated from chemical reactions solely. This work has shown that:

1. In the generation of NCl, the branching ratio for NCl(a) is high. 65% of the HN_3 ends up in in the NCl(a) state.
2. The rate constant for the energy-pooling reaction NCl(a) + I* $\rightarrow$ NCl(b) is quite favorably large, approximately 10^{-11} cm^3/sec.
3. A gain on the order of $1 \times 10^{-4} cm^{-1}$ was obtained.
4. Variations of the cavity ring-down experiment showed that virtualy no NCl(X) is formed via reaction (2.6)

7. REFERENCES

1. J. M. Herbelin, M. A. Kwok, and D. J. Spencer, "Enhancement of NF($b^1\Sigma$) by Iodine Laser Pumping," J. Appl. Phys. 49, 3750. (1978)

2. J. M. Herbelin, "Prospects of a Visible (Green) Chemical Laser," Appl. Opt., 25, 2138. (1986)

3. G. P. Perram, "Overview of Excited NF Driven Laser Program for SDIO/T/DE," Atlanta, GA, 4-.5. (April 1989)

4. D. R. Yarkony, "A Theoretical Description of the Radiative Decay Processes ($b^1\Sigma$, $a^1\Delta$) $\rightarrow$ $X^3\Sigma$ in NF," J. Chem. Phys. 85, 7261 (1986).

5. J. Herbelin, "Electronic Energy Transfer Between NF(b) and IF(x)," Chem. Phys. Letters, 133, 331. (1987)

6. A. T. Pritt, Jr., and D. J. Benard, "Temperature Dependence of the Rate of the Electronic-to-Electronic Energy Transfer from NF($b^1\Sigma$) to IF," J. Chem. Phys. 85, 7159. (1986)

7. H. Cha and D. W. Setser, "NF(b1S) Quenching Rate Constants by Fadrogens and Interhalogens, and the Excitation Rate Constant for IF(B) Formation," J. Phys. Chem. 91, 3758. (1987)

8. I. Barnes, K. H. Becker, and E. H. Fink, "Near-Infrared Emissions From the $^1\Delta g$ and $^1\Sigma g+$ states of Σ_2," Chem. Phys. Letters 67, 314. (1979

9. P. V. Avizonis, "Chemically Pumped Electronic Transition Lasers," Gas Flow and Chemical Lasers, Ed. M. Onorato, Plenum Press, N.Y.

10. D. R. Yarkony, "On the Radiative Lifetimes of the $b^1\Sigma$ and $a^1\Delta$ states in NCl," J. Chem. Phys., 86, 1649. (1987)

11. P. V. Avizonis and D. K. Neumann, "The Chemical Oxygen-Iodine Laser,"AFWL Report, unpublished. (1986)

12. A. T. Pritt, Jr., D. Patel, and R. D. Coombe, "Yields of Singlet Nitrenes from Halogen Atom-Azide Molecule Reactions," Int. J. Chem. Kinet, 16, 977. (1984)

13. M. A. A. Clyne, A. J. Macroberrt, J. Brunning, and C. T. Cheah, "Kinetics of Metastable Singlet NCl Radicals," J. Chem. Soc., Faraday Trans. 2, 79 (1515. (1983)

14. R. D. Bower and T. T. Yang, "I($^2P_{1/2}$) produced by the energy transfer from NCl($a^1\Delta$) to I($^2P_{3/2}$)," J. Opt. Soc. Am B 8, 1583. (1991)

15. T. T. Yang and R. D. "Bower, Excitation of I($^2P_{1/2}$) by NCl($a^1\Delta$)," SPIE Proceedings, Vol. 1225, High Power Gas Lasers, 430. (1990)

16. T. T. Yang and V. T. Gylys, "Short Wavelength Chemical Laser Developments," Rocketdyne IR&D Technical Report ITR-91-130, Oct. 10, 1991.

17. A. T. Pritt, Jr., D. Patel, and R. D. Coombe, "Visible and Near-Infrared Electronic Transitions in NCl and NBr," J. Mol. Spectrosc. 87, 401. (1981)

18. T. C. Clark and M. A. Clyne, Trans. Faraday Soc., 66, 877. (1970)

19. G. A. Woolsey, P. A. Lee and W. D. Shater, J. Chem. Phys., 67, 1220. (1977)

20. A. J. Ray and R. D. Coombe, J. Chem. Phys., 97, 3475. (1993)

21. A. O'Keefe and D. A. Deacon, Rev. Sci. Instr., 59, 2544. (1988)

	ν (cm^{-1})	τ_R	ωe (cm^{-1})	σ (cm^2)	λ (nm)
NF ($a^1\Delta$)	11435	5.6 s	1184	10^{-22}	874.2
NF ($b^1\Sigma$)	18905	20 ms	1197	10^{-19}	528.8
NCl ($a^1\Delta$)	9260	1.4 s	904	2×10^{-21}	1080
NCl ($b^1\Sigma$)	14984.6	630 μs	935.6	3×10^{-18}	665
NI ($a^1\Delta$)	8440 (8520)	< 1 s	595	10^{-20}	1174
NI ($b^1\Sigma$)	13419	15 μs	703	2×10^{-17}	745
IF (B)	19054	7 μs	406.5	$\sim 10^{-16}$	625
BIF (A)	22956.98	1.4 μs	384	8×10^{-17}	471
O_2 (a)	7882	45 min	1509	$< 10^{-25}$	1269
I ($^2P_{1/2}$)	7603	0.18 s		7.4×10^{-18}	1315
O_2 (b)	13121	13 s			760

Table 2.1 Radiative Lifetimes, Gain Cross Sections, and Emission Wavelengths for various possible chemical laser candidates.

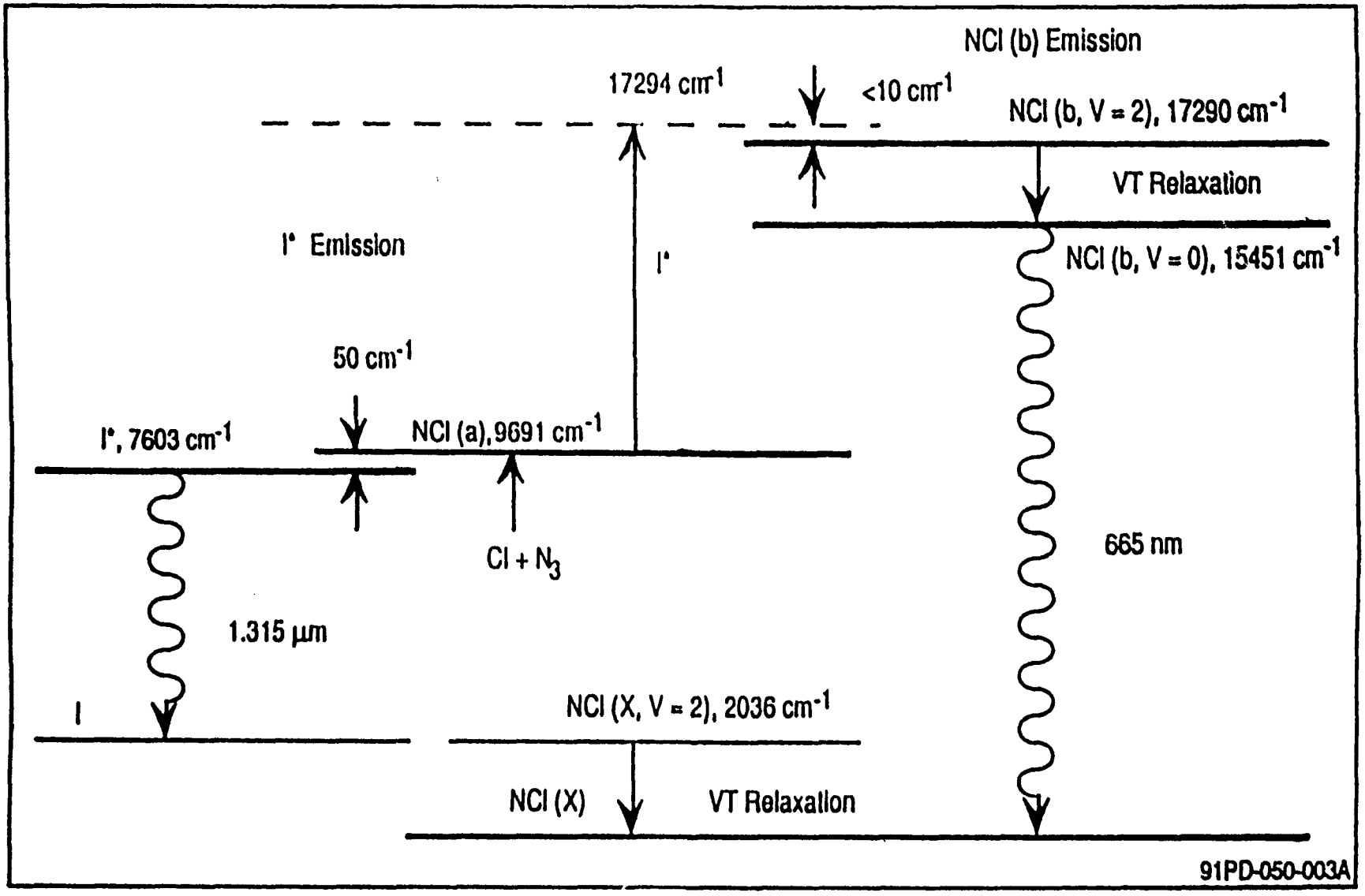

Figure 2.1 Energy diagram showing pumping scheme for I* and NCl(b).

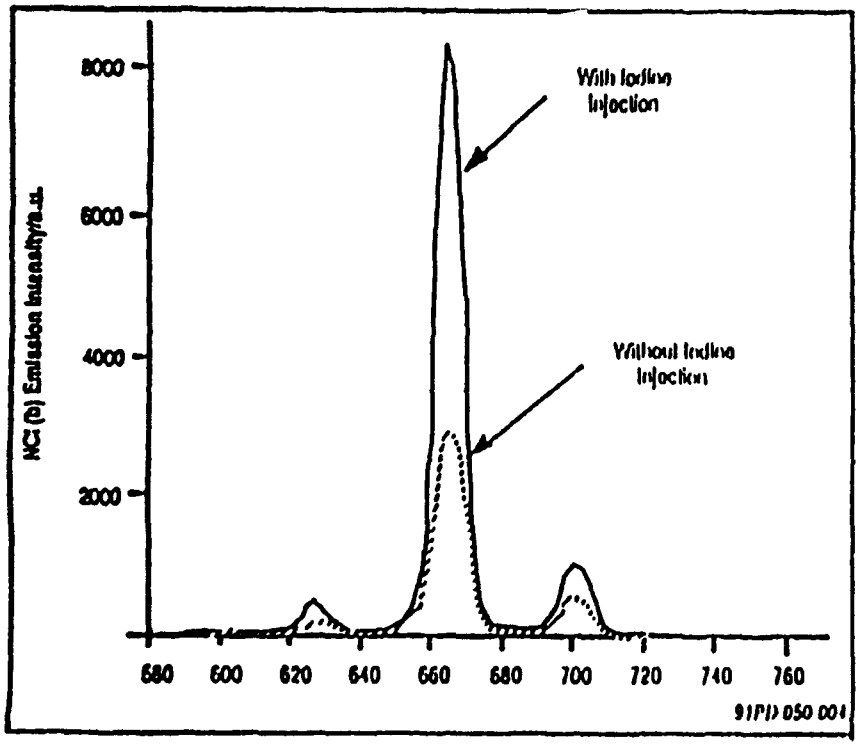

Figure 2.2 NCl(b) Visible Emission with and without Iodine Injection

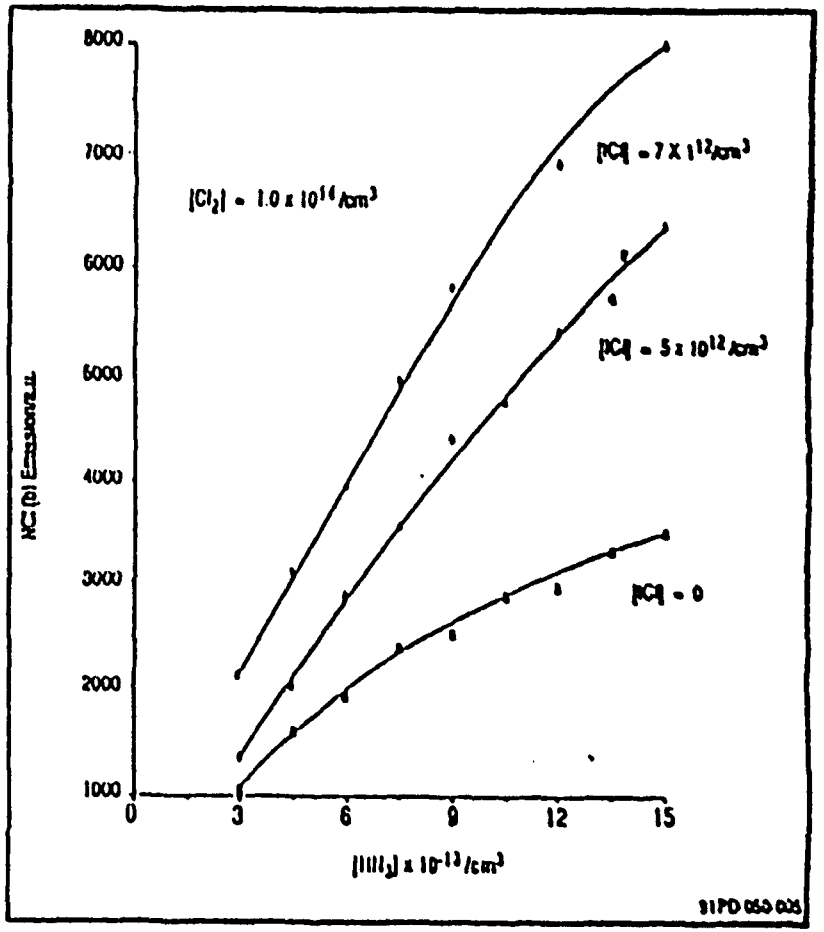

Figure 2.3 I* Enhanced NCl(b) Emission.

Table 3.1 Values of the rate constant for NO - O chemiluminescence at several wavelengths.

$\lambda(\mu m)$	$K_c(10^{-17} cm^3\ s^{-1} \mu m^{-1})$
0.54	6.1 + 1.8
0.60	7.9 + 2.0
0.70	7.1 + 1.8
0.80	6.0 + 1.5
0.90	5.2 + 1.6
0.95	4.8 + 1.2
1.05	3.7 + 1.0
1.15	2.8 + 0.8
1.27	1.8 + 0.8

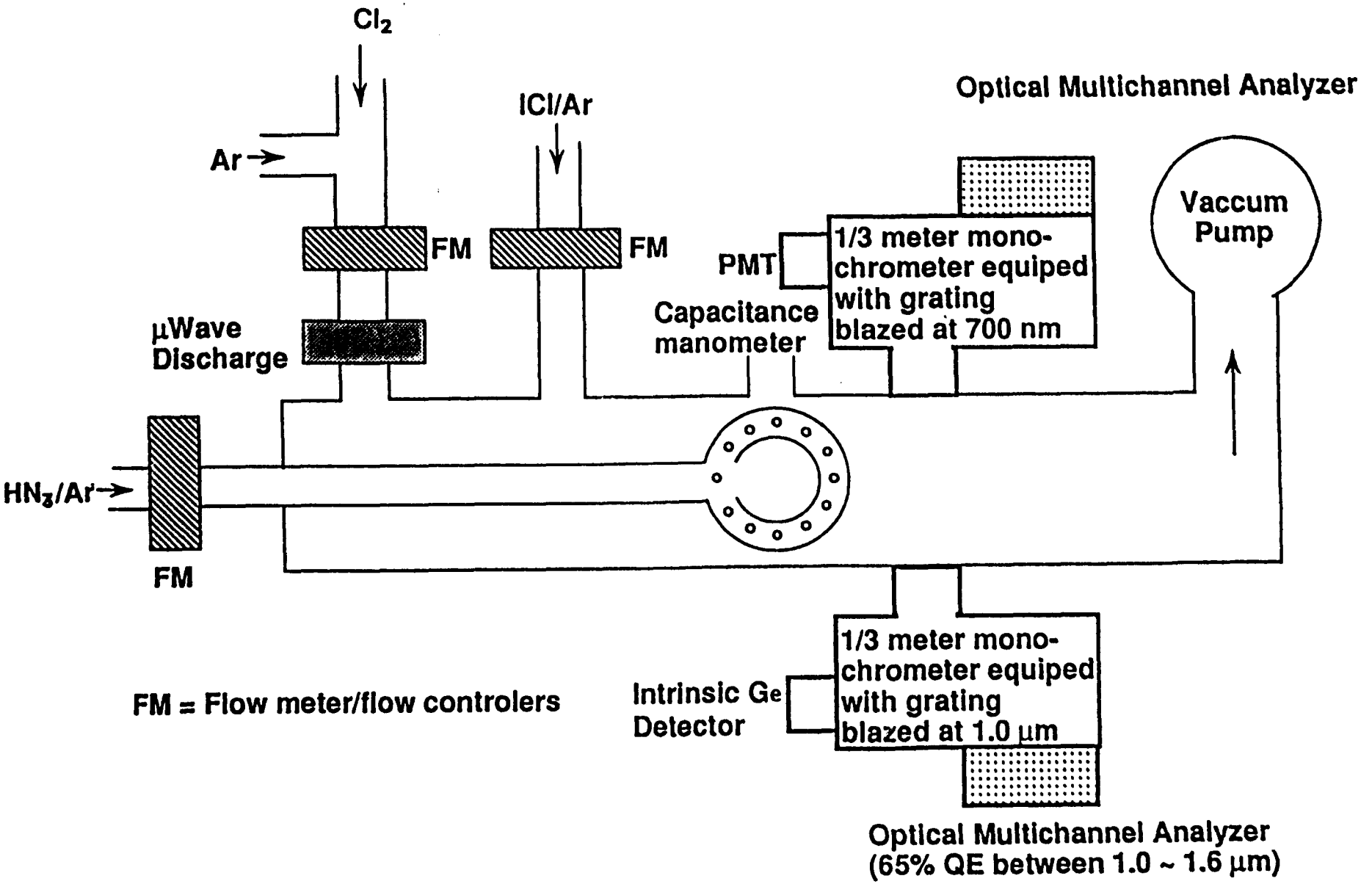

Figure 3.1 Schematic of experimental setup used to make photon yield measurements and derive the I^*-NCl(a) pooling rate.

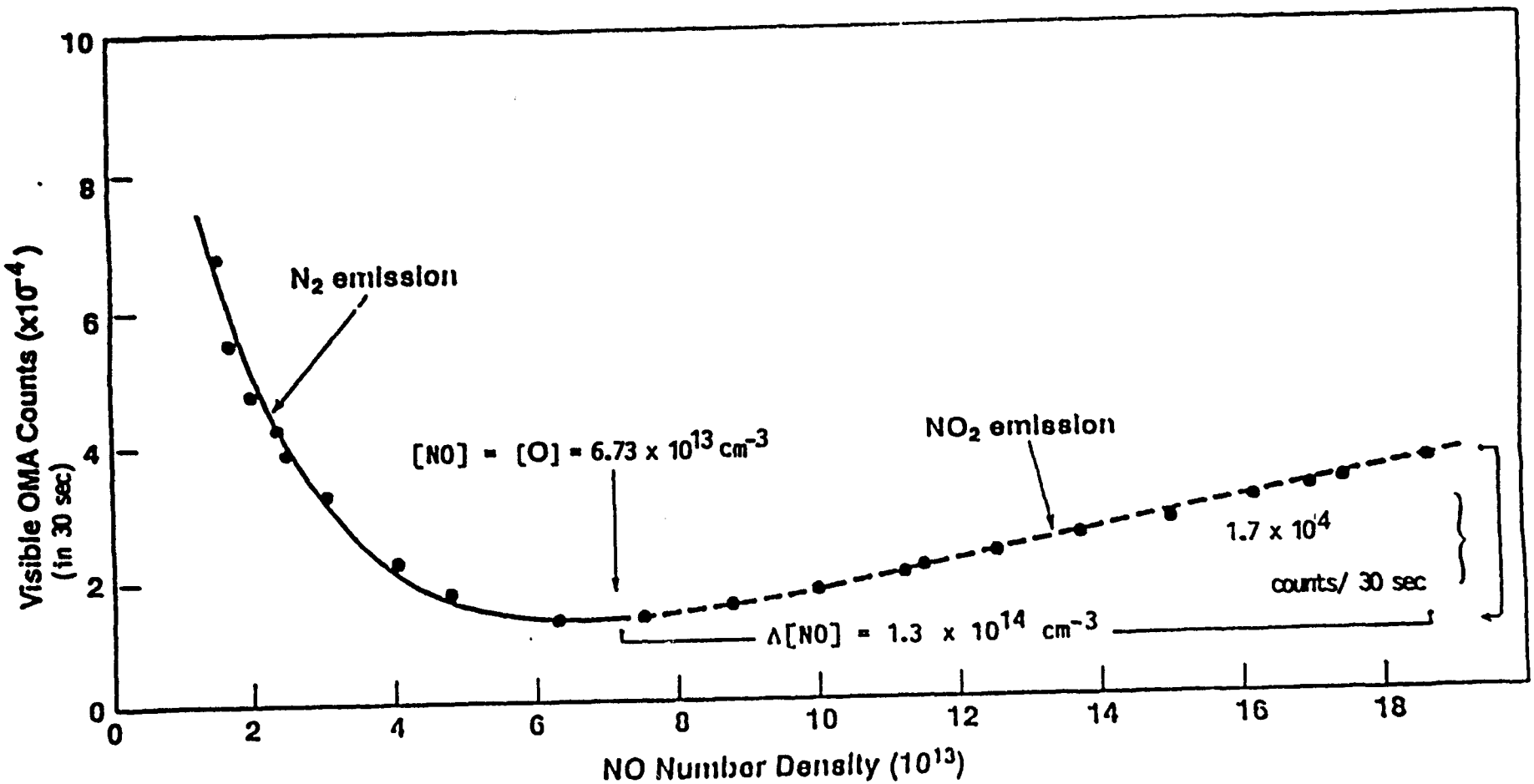

Figure 3.2 Calibration of visible OMA using NO + O recombination as a chemical actinometer.

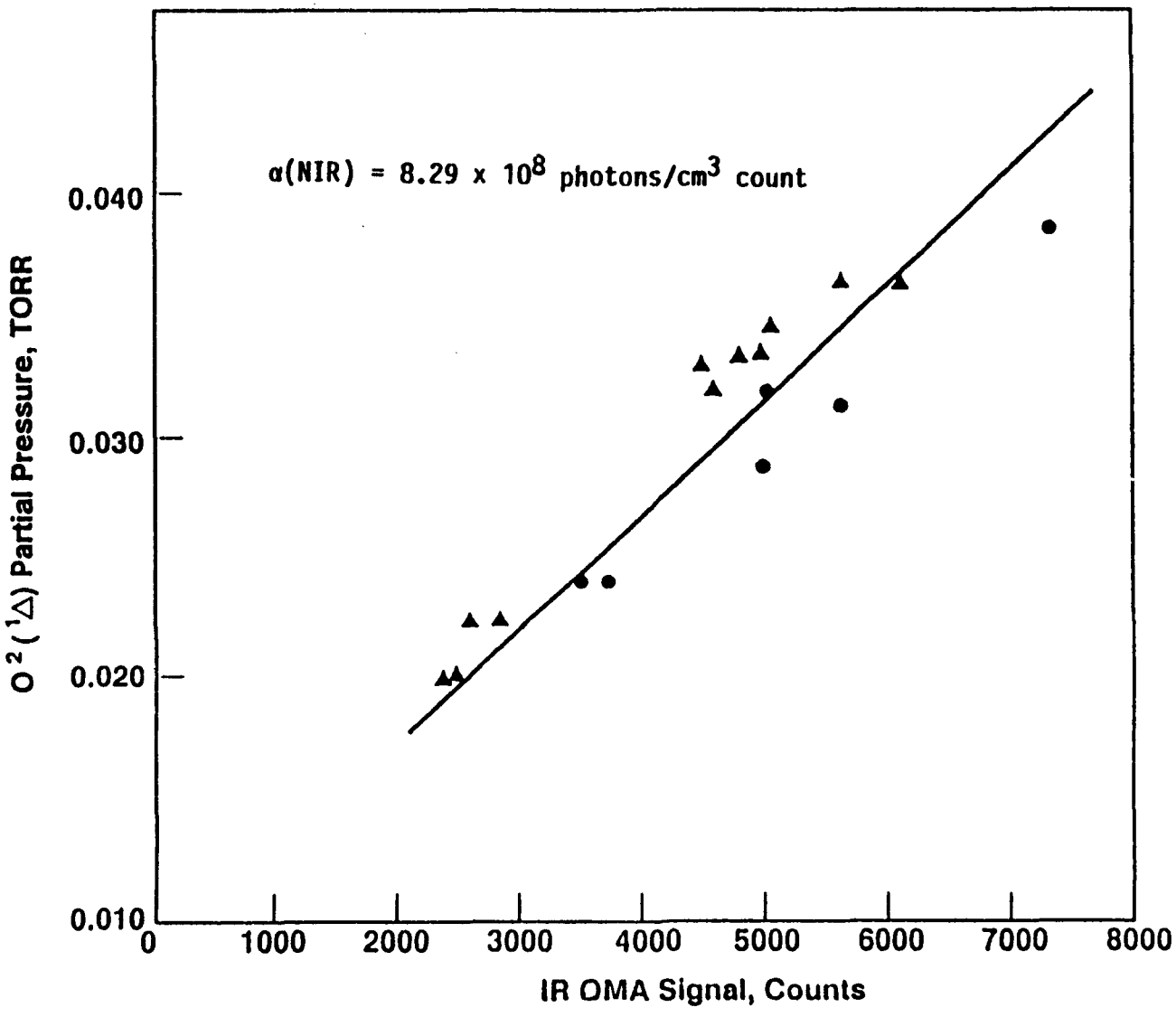

Figure 3.3 Absolute calibration of IR OMA using electron spin resonance to determine the number density of $O_2{}^1\Delta$. The triangles and dots represent data accumulated during two separate experiments. The slope of the line indicates that $\alpha(NIR) = 8.29 \times 10^8$ photons/cm^3 count.

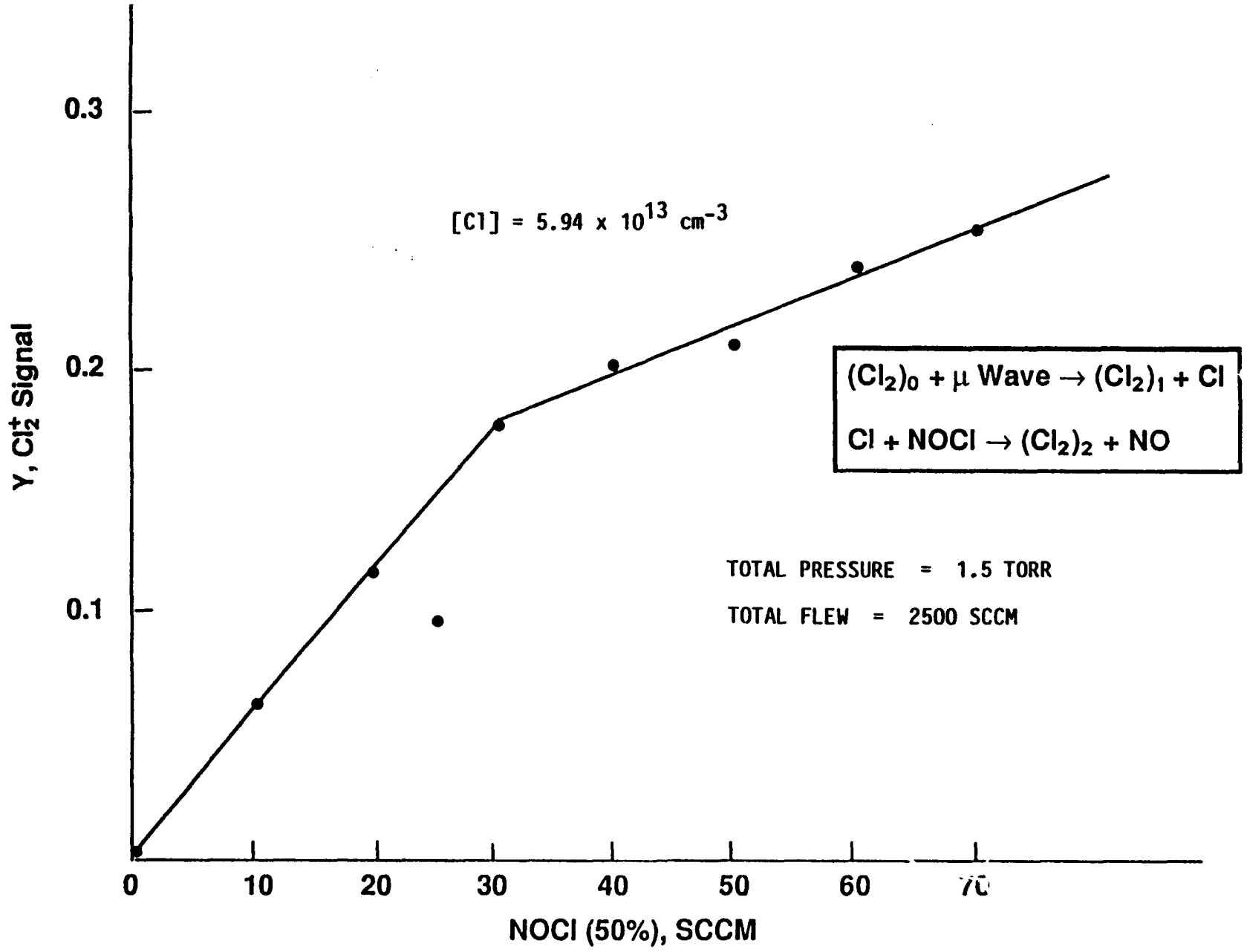

Figure 3.4 Determination of [Cl] using Mass Spectrometer.

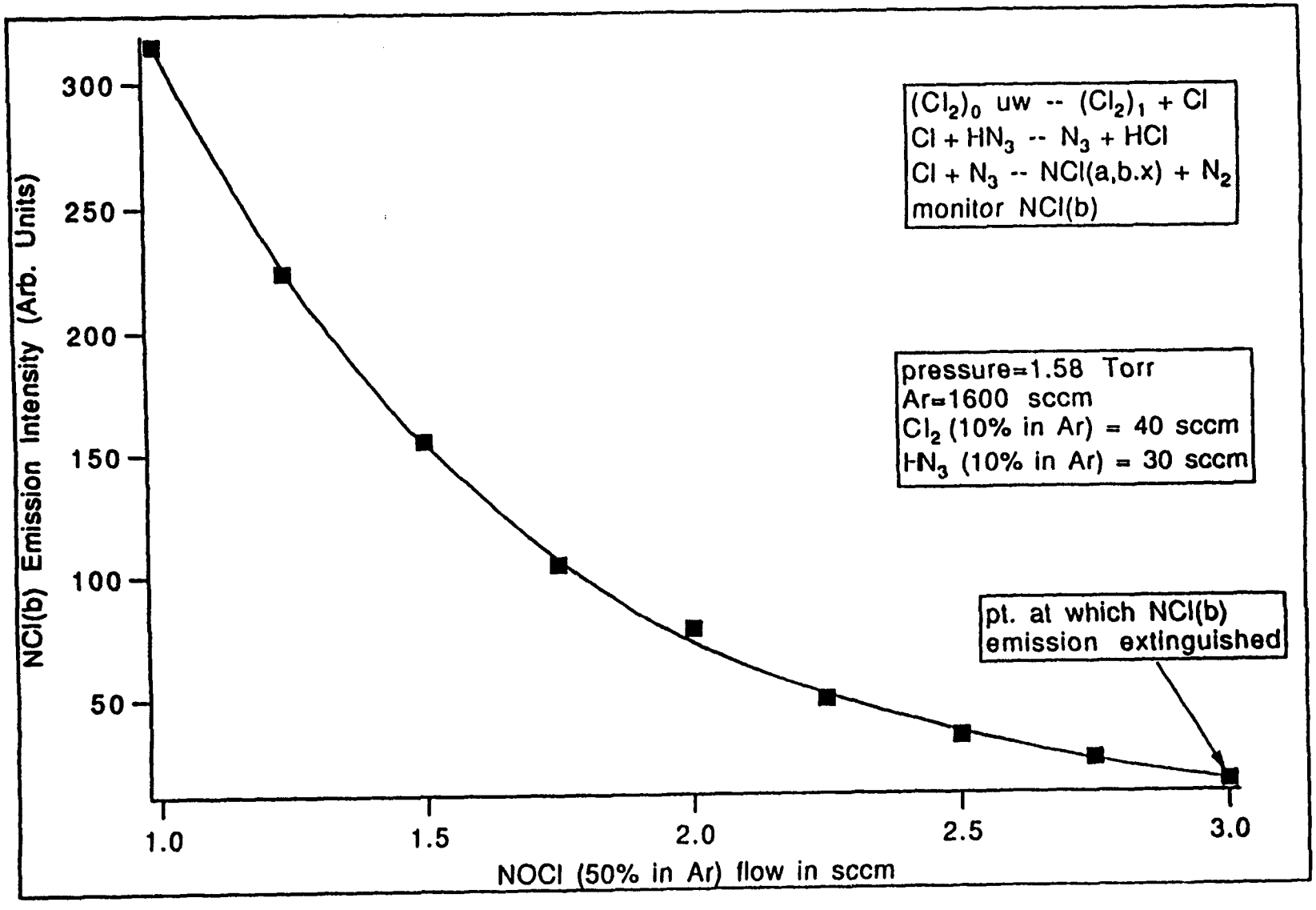

Figure 3.5 Titration of Cl with NOCl by monitoring the decrease of the NCl(b-X) emission at 665 nm. The NCl(b) emission is extinguished at a NOCl(50% in Ar) flow rate of 3.0 sccm. The total flow in the CFFR was 1673 sccm and the total pressure was 1.58 Torr. This indicates that [Cl] = 4.6×10^{13} cm^{-3}.

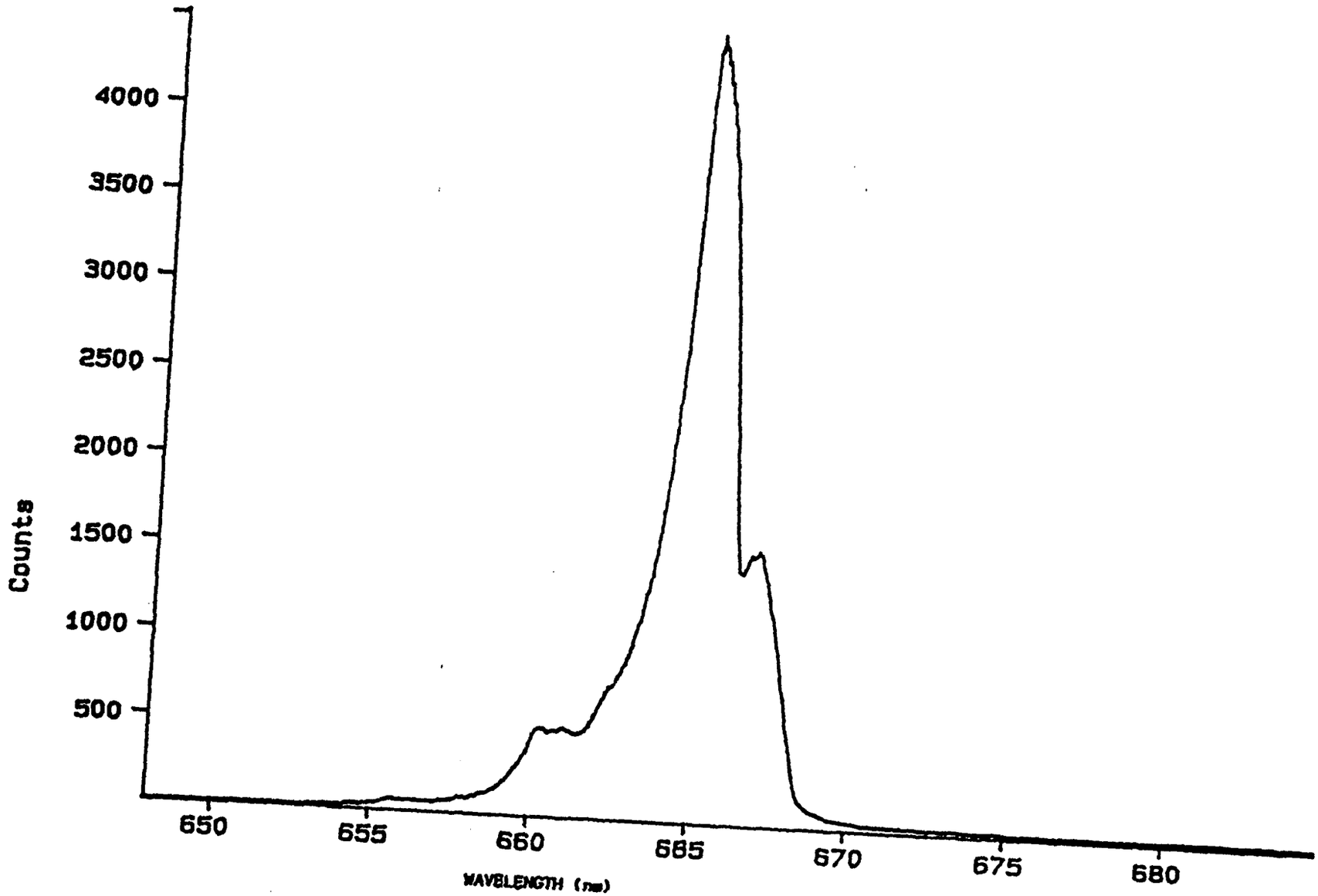

Figure 3.6a Typical NCl(b→ X) emission spectrum obtained 11cm downstream of HN_3 injector.

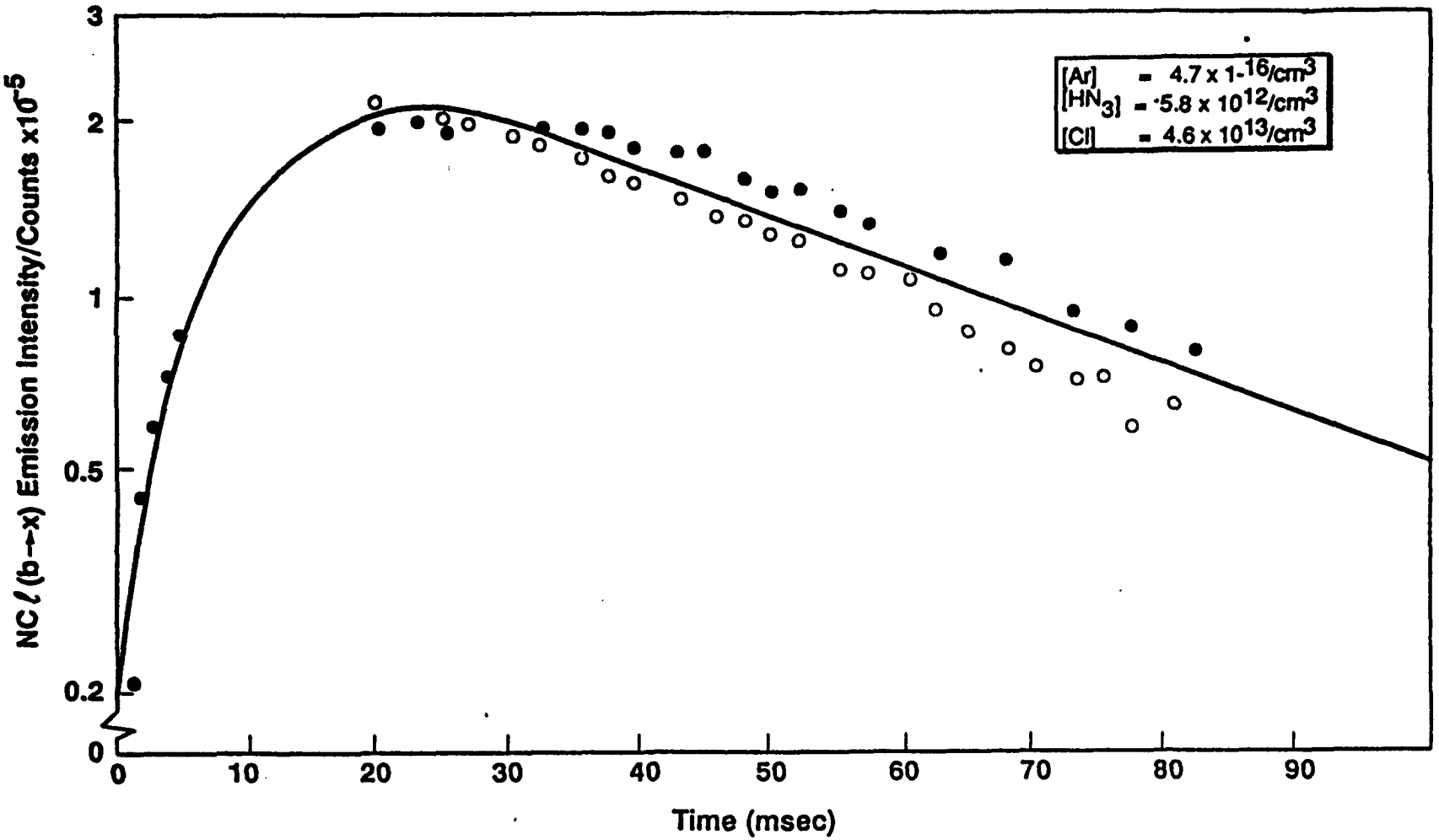

Figure 3.6b The build-up and decay of NCl(b) fluorescence intensity at 665 nm as a function of flow time from the point of HN_3 injection. The open and closed circles represent data points taken under identical conditions in two separate tests.

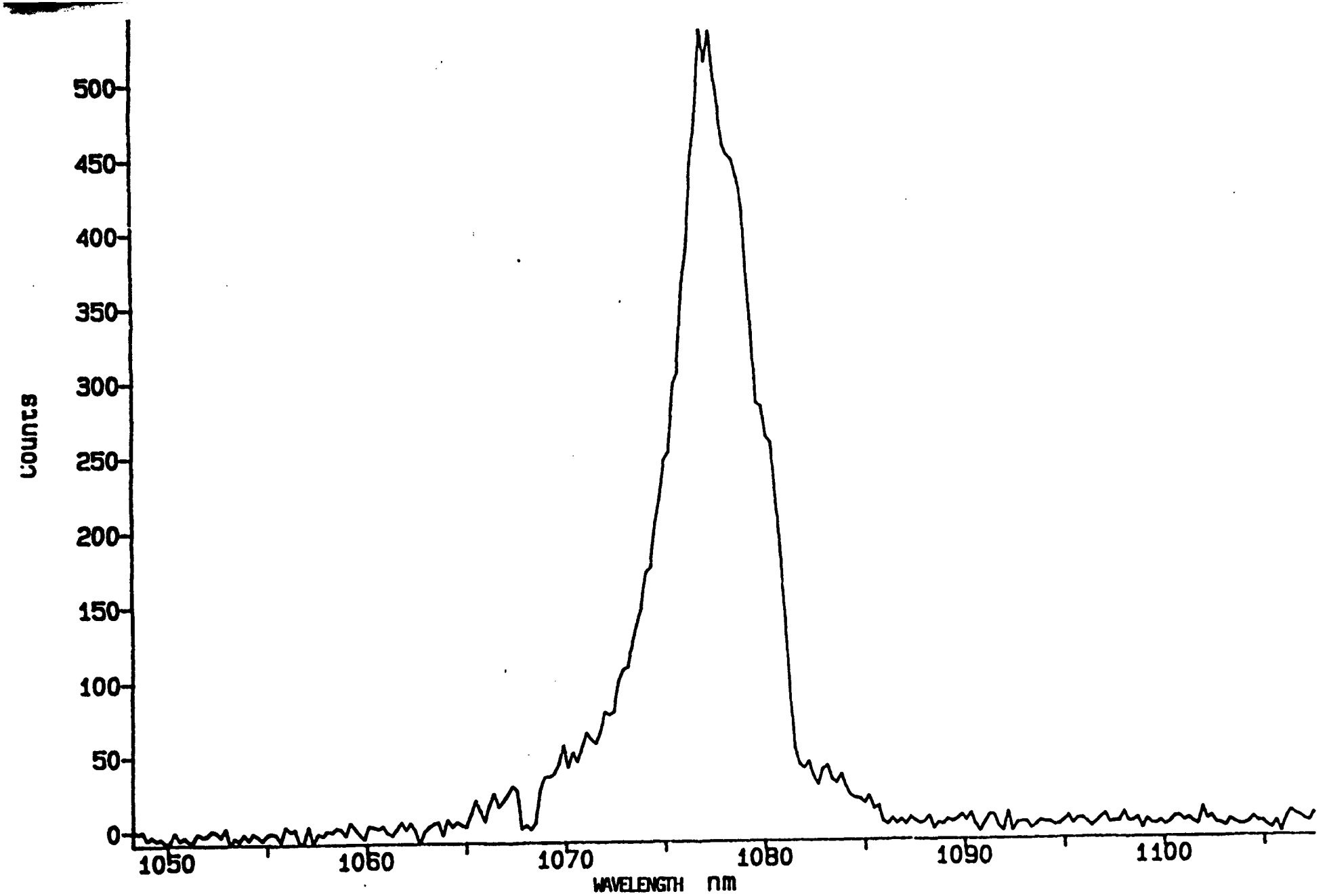

Figure 3.7a Typical NCl(a→ X) emission spectrum obtained 11cm downstream of HN_3 injector.

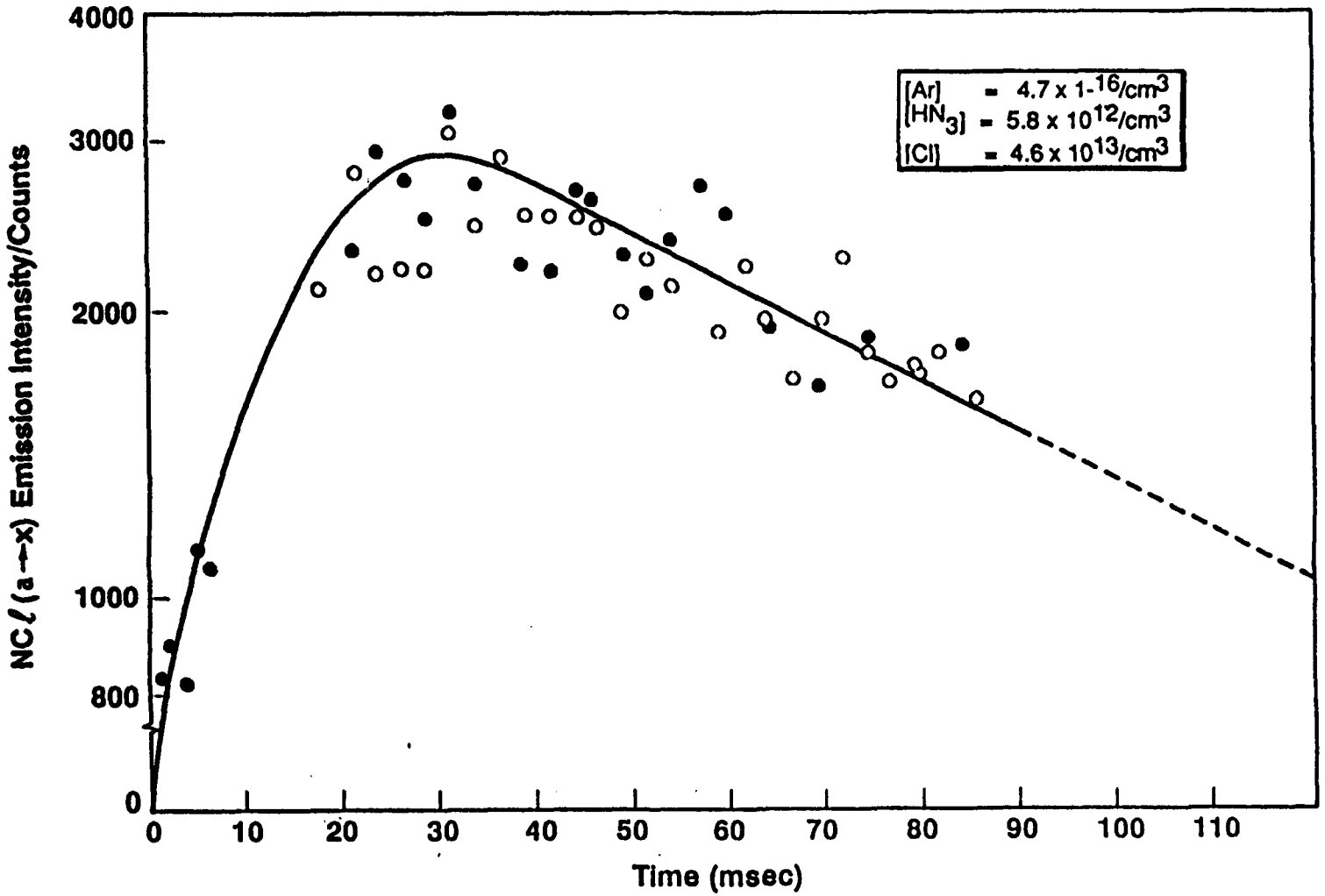

Figure 3.7b The build-up and decay of NCl(a) fluorescence intensity at 1.08 μm as a function of flow time from the point of HN_3 injection. The open and closed circles represent data points taken under the same conditions in two separate tests.

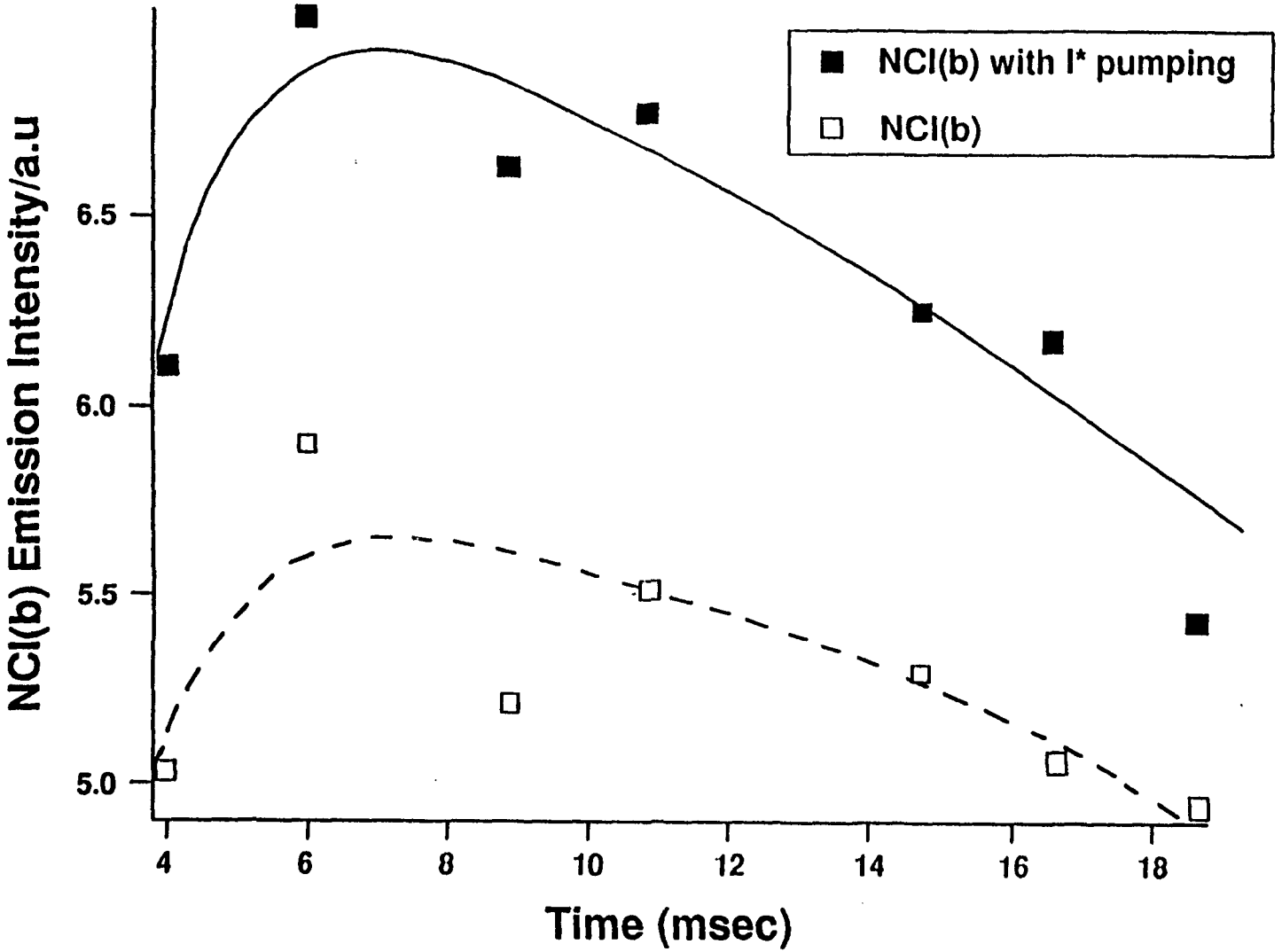

Figure 4.1 *Time decay of* NCl(b) emission at 665 nm with and without the presence of I.

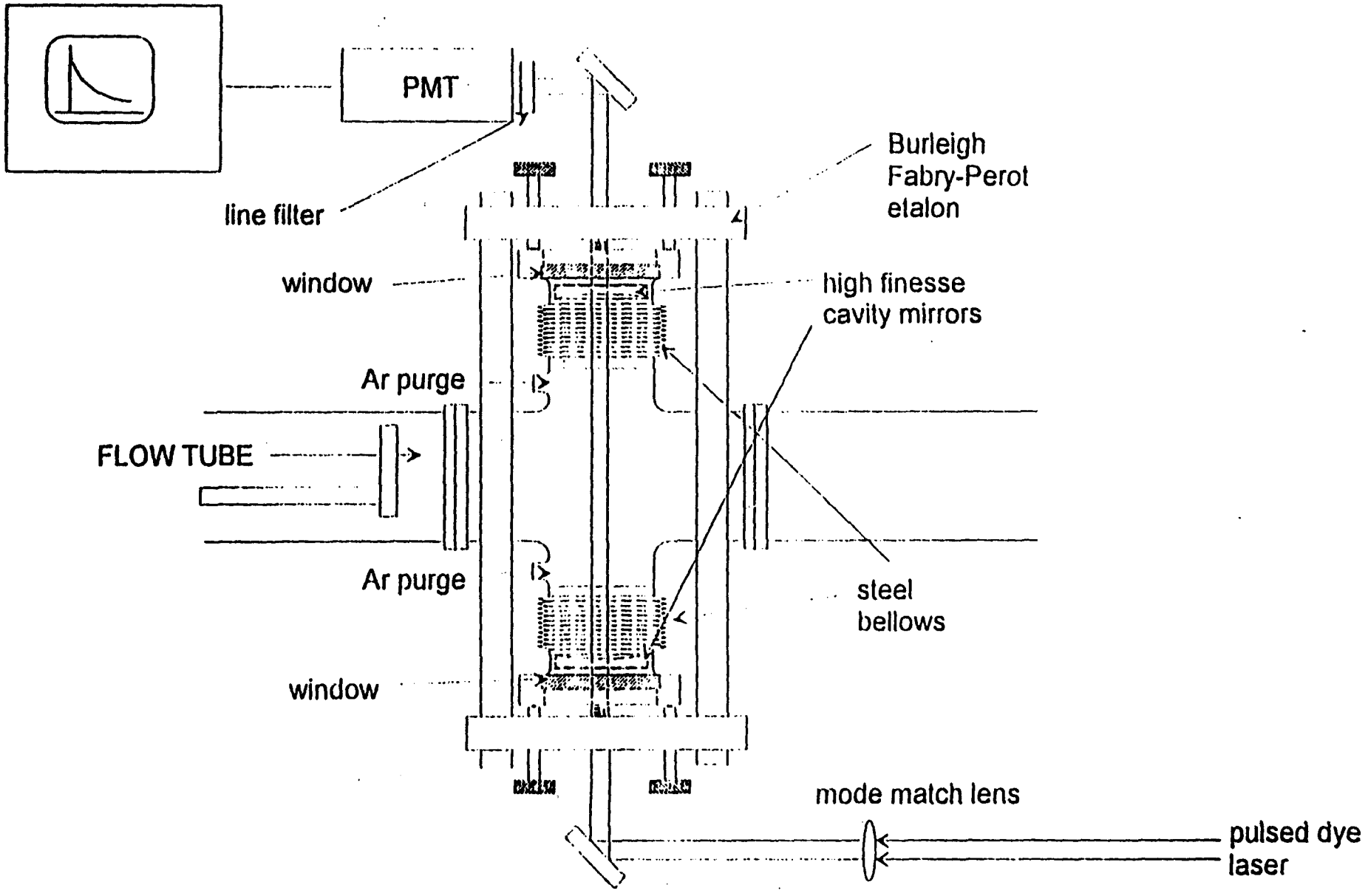

Figure 5.1 Schematic of the experimental setup used for the cavity ring-down gain measurement.

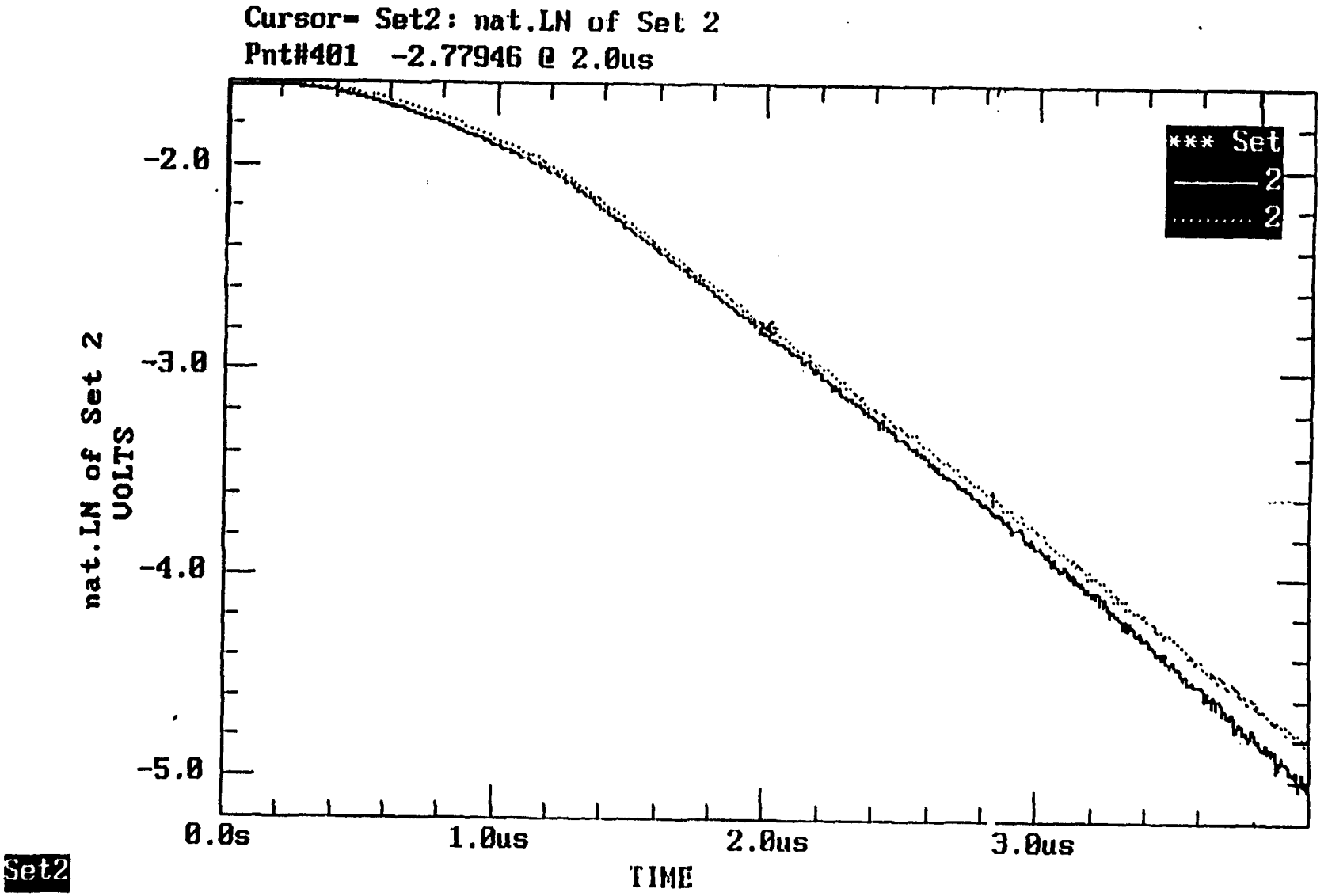

Figure 5.2 Oscilloscope traces of cavity decay: Lower trace - without NCl present; upper trace - with NCl present